Progress In Electromagnetics Research, PIER 86, 199–215, 2008

NOVEL BLIND JOINT DIRECTION OF ARRIVAL AND FREQUENCY ESTIMATION FOR UNIFORM LINEAR ARRAY

X. Zhang, D. Wang, and D. Xu

Department of Electronic Engineering
Nanjing University of Aeronautics & Astronautics
Nanjing 210016, China

Abstract—This paper links joint direction of arrival (DOA) and frequency estimation problem to the trilinear model and derives a novel blind joint angle and frequency estimation algorithm. The proposed algorithm has better performance than ESPRIT algorithm. Our proposed algorithm is thought of as a generalization of ESPRIT. The useful behavior of the proposed algorithm is verified by simulations.

1. INTRODUCTION

Antenna array has been used in many fields such as radar, sonar, communications, seismic data processing, and so on [1–12]. The direction-of-arrival (DOA) estimation [13–19] of signals impinging on an array of sensors is a fundamental problem in array processing. The problem of joint DOA and frequency estimation arises in the applications of radar, wireless communications. For example, these parameters can be applied to locate the mobiles and to allocate pilot tones in space division multiple access systems. Furthermore, a precise estimation of these parameters is helpful to attain a better channel estimate and thus enhances the system performance. Optimal techniques based on maximum likelihood [20] are often applicable but might be computationally prohibitive. Some ESPRIT-based joint angle and frequency estimation methods have been proposed in [21–27]. Zoltowski [21] discusses this problem in the context of radar applications. Pro-ESPRIT is proposed to estimate angle and frequency. Haardt [22] discusses the problem in the context of mobile communications for space division multiple access applications. Their method is based on Unitary-ESPRIT, which involves a certain transformation of the data to real valued matrices. Multi-resolution

ESPRIT is used for joint angle frequency estimation in [23]. ESPRIT method is used for frequency and angle estimation under uniform circular array in [25, 26]. The others joint angle and frequency estimation method is proposed in [28, 29]. ESPRIT method algorithm requires eigen-value decomposition (EVD) to the cross spectral matrix or singular value decomposition (SVD) to the received data. EVD or SVD needs high computational complexity. ESPRIT ideas have revolutionized sensor array signal processing. Interestingly, a general principle underlying ESPRIT has flourished independently in other scientific fields and disciplines, where it is commonly referred to in a variety of ways, including trilinear model or trilinear decomposition. Trilinear decomposition-based joint angle and frequency estimation for uniform linear array is investigated in this paper.

It was known that most of signal processing methods are based on the theory of matrix, or the bilinear model. In general, matrix decomposition is not unique, since inserting a product of an arbitrary invertible matrix and its inverse in between two matrix factors preserves their product. Matrix decomposition can be unique only if one imposes additional problem-specific structural properties including orthogonality, Vandermonde, Toeplitz, constant modulus or finite-alphabet constraints. Compared to the case of matrices, trilinear model or trilinear decomposition has a distinctive and attractive feature: it is often unique [30]. The uniqueness of trilinear decomposition is of great practical significance, which is crucial in many applications such as psychometrics [31] and chemistry [32–34]. Trilinear decomposition is thus naturally related to linear algebra for multi-way arrays. Trilinear decomposition in signal processing fields can be thought of as a generalization of ESPRIT and joint approximate diagonalization ideas [35, 36].

Our work links the uniform linear array parameter estimation problem to the trilinear model and derives a novel blind angle and frequency estimation algorithm. The proposed algorithm has better performance than ESPRIT, and supports small sample sizes. This method relies on a fundamental result of Kruskal [30] regarding the uniqueness of low-rank three-way data decomposition. This method is an iterative algorithm, which does not need EVD or SVD, and only requires fewer iterations for convergence.

This paper is structured as follows. Section 2 develops data model. Section 3 deals with trilinear decomposition and discusses identifiability issues. The blind joint angle and frequency estimation method is proposed in Section 4. Section 5 presents simulation results. Section 6 summarizes our conclusions.

Denote: We denote by $(.)^*$ the complex conjugation, by $(.)^T$ the matrix transpose, and by $(.)^H$ the matrix conjugate transpose. The notation $(.)^+$ refers to the Moore-Penrose inverse (pseudo inverse). $\| \|_F$ stands for Frobenious norm.

2. THE DATA MODEL

There are K sources to reach uniform linear array with M elements. Suppose that the ith source has a carrier frequency of f_i. The signal received at the mth antenna is

$$x_m(t) = \sum_{i=1}^{K} e^{j2\pi(m-1)df_i \sin(\theta_i)/c} s_i(t) \tag{1}$$

where θ_i is direction of arrival (DOA) of the ith signal, d is array spacing. $s_i(t)$ is the narrow-band signal of the ith source.

In order to estimate frequency, we add the delayed outputs $\tau_p, p = 1, 2, \ldots, P$ for the received signal of array antenna, as shown in Fig. 1. We suppose that $0 < \tau_1 < \tau_2 < \ldots < \tau_P < 1/\max(f_i)$.

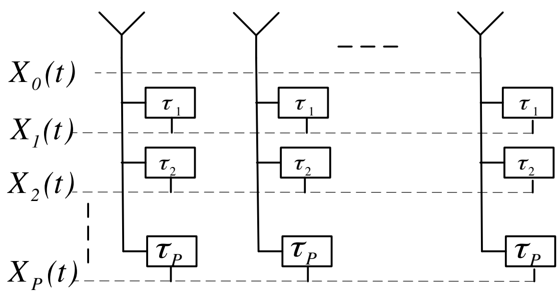

Figure 1. The received signal with delayed output.

The delayed signal for (1) with delay τ_p is

$$\begin{aligned} x_m(t-\tau_p) &= \sum_{i=1}^{K} e^{j2\pi(m-1)df_i \sin(\theta_i)/c} s_i(t-\tau_p) \\ &= \sum_{i=1}^{K} e^{j2\pi(m-1)df_i \sin(\theta_i)/c} s_i(t) e^{-j2\pi f_i \tau_p} \end{aligned} \tag{2}$$

where c is velocity of light.

We assume that channel state information is constant for N symbols. The received signal of array antennas can be denoted as

$$\mathbf{X}_0(t) = \mathbf{AS} \tag{3}$$

where the source matrix $\mathbf{S}$ and the direction matrix $\mathbf{A}$ are shown as follows

$$\mathbf{S} = \begin{bmatrix} \mathbf{s}_1 & \mathbf{s}_2 & \cdots & \mathbf{s}_K \end{bmatrix}^T \in \mathbb{C}^{K \times N} \tag{4}$$

$$\mathbf{A} = \begin{bmatrix} 1 & 1 & \cdots & 1 \\ e^{-\frac{j2\pi d f_1 \sin\theta_1}{c}} & e^{-\frac{j2\pi d f_2 \sin\theta_2}{c}} & \cdots & e^{-\frac{j2\pi d f_K \sin\theta_K}{c}} \\ \vdots & \vdots & \ddots & \vdots \\ e^{-\frac{j2\pi (M-1) d f_1 \sin\theta_1}{c}} & e^{-\frac{j2\pi d (M-1) f_2 \sin\theta_2}{c}} & \cdots & e^{-\frac{j2\pi d (M-1) f_K \sin\theta_K}{c}} \end{bmatrix} \in \mathbb{C}^{M \times K} \tag{5}$$

The delayed signal for (3) with τ_p can be denoted as

$$\mathbf{X}_p = \mathbf{A}\mathbf{\Phi}_p\mathbf{S} \tag{6}$$

where

$$\mathbf{\Phi}_p = \begin{bmatrix} e^{-j2\pi f_1 \tau_p} & & \\ & e^{-j2\pi f_2 \tau_p} & \\ & & e^{-j2\pi f_K \tau_p} \end{bmatrix} \in \mathbb{C}^{K \times K} \tag{7}$$

Define the delay matrix as

$$\mathbf{\Phi} = \begin{bmatrix} 1 & 1 & \cdots & 1 \\ e^{-j2\pi f_1 \tau_1} & e^{-j2\pi f_2 \tau_1} & \cdots & e^{-j2\pi f_K \tau_1} \\ \vdots & \vdots & \ddots & \vdots \\ e^{-j2\pi f_1 \tau_P} & e^{-j2\pi f_2 \tau_P} & \cdots & e^{-j2\pi f_K \tau_P} \end{bmatrix} \in \mathbb{C}^{P+1 \times K} \tag{8}$$

Eq. (6) is also denoted as

$$\mathbf{X}_p = \mathbf{A}D_{p+1}(\mathbf{\Phi})\mathbf{S}, \ \ p = 0, 1, \ldots, P \tag{9}$$

where $D_m(.)$ is to extract the mth row of its matrix argument and constructs a diagonal matrix out of it. When $p = 0$, $\mathbf{X}_p|_{p=0} = \mathbf{X}_0$, that is to say, $\tau_p|_{p=0} = 0$.

In the presence of noise, the received signal model becomes

$$\tilde{\mathbf{X}}_p = \mathbf{X}_p + \mathbf{W}_p = \mathbf{A}D_{p+1}(\mathbf{\Phi})\mathbf{S} + \mathbf{W}_p, \ \ p = 0, 1, \ldots, P \tag{10}$$

where $\mathbf{W}_p$, the $M \times N$ matrix, is the received noise corresponding to the pth slice.

The signal in (9) is also denoted through rearrangements

$$x_{m,n,p} = \sum_{f=1}^{K} a_{m,f} s_{n,f} \phi_{p,f}$$
$$m = 1, \ldots, M; \;\; n = 1, \ldots, N; \;\; p = 0, 1, \ldots, P \tag{11}$$

where $a_{m,f}$ stands for the (m, f) element of $\mathbf{A}$ matrix, and similarly for the others. The signal in (11) is a sum of triple products; it is well known as the trilinear model or trilinear decomposition. The trilinear model $\mathbf{X}$ reflects three different kinds of diversity available: spatial, temporal and delay diversity. Another view, $\mathbf{X}_p = \mathbf{A}D_{p+1}(\mathbf{\Phi})\mathbf{S}$, $p = 0, 1, \ldots, P$, can be interpreted as slicing the 3-D data in a series of slices (2-D data) along the spatial direction. Meanwhile, the symmetry of the trilinear model in (11) allows two more matrix system rearrangements, for which we have

$$\mathbf{Y}_n = \mathbf{\Phi} D_n \left(\mathbf{S}^T\right) \mathbf{A}^T, \;\; n = 1, 2, \ldots, N \tag{12}$$

where $\mathbf{Y}_n$ is the nth slice in the temporal direction. Similarly

$$\mathbf{Z}_m = \mathbf{S}^T D_m(\mathbf{A}) \mathbf{\Phi}^T, \;\; m = 1, 2, \ldots, M \tag{13}$$

where $\mathbf{Z}_m$ is the pth slice in spatial direction.

3. TRILINEAR MODEL AND ITS DECOMPOSITION

3.1. Trilinear Decomposition

TALS (Trilinear Alternating Least Square) algorithm is the common data detection method for trilinear model [30]. The basic idea of TALS is as follows: (a) Each time, update a matrix using least squares conditioned on previously obtained estimates of the remaining matrix; (b) proceed to update another matrix; (c) repeat until convergence. TALS algorithm is discussed in detail as follows.

According to (9), it is rewritten as

$$\begin{bmatrix} \mathbf{X}_0 \\ \mathbf{X}_1 \\ \vdots \\ \mathbf{X}_P \end{bmatrix} = \begin{bmatrix} \mathbf{A}D_1(\mathbf{\Phi}) \\ \mathbf{A}D_2(\mathbf{\Phi}) \\ \vdots \\ \mathbf{A}D_{P+1}(\mathbf{\Phi}) \end{bmatrix} \mathbf{S} \tag{14}$$

Least squares (LS) fitting is

$$\min_{\mathbf{A},\mathbf{S},\mathbf{\Phi}} \left\| \begin{bmatrix} \tilde{\mathbf{X}}_0 \\ \tilde{\mathbf{X}}_1 \\ \vdots \\ \tilde{\mathbf{X}}_P \end{bmatrix} - \begin{bmatrix} \mathbf{A}D_1(\mathbf{\Phi}) \\ \mathbf{A}D_2(\mathbf{\Phi}) \\ \vdots \\ \mathbf{A}D_{P+1}(\mathbf{\Phi}) \end{bmatrix} \mathbf{S} \right\|_F \tag{15}$$

where $\| \, \|_F$ stands for the Frobenius norm. $\tilde{\mathbf{X}}_p, p = 0, 1, \ldots, P$ are the noisy slices.

Least squares update for $\boldsymbol{S}$ is

$$\hat{\mathbf{S}} = \begin{bmatrix} \hat{\mathbf{A}}D_1\left(\hat{\mathbf{\Phi}}\right) \\ \hat{\mathbf{A}}D_2\left(\hat{\mathbf{\Phi}}\right) \\ \vdots \\ \hat{\mathbf{A}}D_{P+1}\left(\hat{\mathbf{\Phi}}\right) \end{bmatrix}^+ \begin{bmatrix} \tilde{\mathbf{X}}_0 \\ \tilde{\mathbf{X}}_1 \\ \vdots \\ \tilde{\mathbf{X}}_P \end{bmatrix} \tag{16}$$

where $[.]^+$ stands for pseudo-inverse. $\hat{\mathbf{A}}$ and $\hat{\mathbf{\Phi}}$ denote previously obtained estimates of $\mathbf{A}$ and $\mathbf{\Phi}$, respectively.

Similarly, from the second way of slices: $\mathbf{Y}_n = \mathbf{\Phi}D_n(\mathbf{S}^T)\mathbf{A}^T$, $n = 1, 2, \ldots, N$, which is rewritten as

$$\begin{bmatrix} \mathbf{Y}_1 \\ \mathbf{Y}_2 \\ \vdots \\ \mathbf{Y}_N \end{bmatrix} = \begin{bmatrix} \mathbf{\Phi}D_1\left(\mathbf{S}^T\right) \\ \mathbf{\Phi}D_2\left(\mathbf{S}^T\right) \\ \vdots \\ \mathbf{\Phi}D_N\left(\mathbf{S}^T\right) \end{bmatrix} \mathbf{A}^T \tag{17}$$

LS fitting is

$$\min_{\mathbf{A},\mathbf{S},\mathbf{\Phi}} \left\| \begin{bmatrix} \tilde{\mathbf{Y}}_1 \\ \tilde{\mathbf{Y}}_2 \\ \vdots \\ \tilde{\mathbf{Y}}_N \end{bmatrix} - \begin{bmatrix} \mathbf{\Phi}D_1\left(\mathbf{S}^T\right) \\ \mathbf{\Phi}D_2\left(\mathbf{S}^T\right) \\ \vdots \\ \mathbf{\Phi}D_N\left(\mathbf{S}^T\right) \end{bmatrix} \mathbf{A}^{TT} \right\|_F \tag{18}$$

where $\tilde{\mathbf{Y}}_n, n = 1, 2, \ldots, N$ are the noisy slices. And the LS update for

$\mathbf{A}$ is

$$\hat{\mathbf{A}}^T = \begin{bmatrix} \hat{\mathbf{\Phi}} D_1\left(\hat{\mathbf{S}}^T\right) \\ \hat{\mathbf{\Phi}} D_2\left(\hat{\mathbf{S}}^T\right) \\ \vdots \\ \hat{\mathbf{\Phi}} D_N\left(\hat{\mathbf{S}}^T\right) \end{bmatrix}^+ \begin{bmatrix} \tilde{\mathbf{Y}}_1 \\ \tilde{\mathbf{Y}}_2 \\ \vdots \\ \tilde{\mathbf{Y}}_N \end{bmatrix} \tag{19}$$

where $\hat{\mathbf{S}}$ and $\hat{\mathbf{\Phi}}$ denote previously obtained estimates of $\mathbf{S}$ and $\mathbf{\Phi}$, respectively.

Finally, from the third way of slices: $\mathbf{Z}_m = \mathbf{S}^T D_m(\mathbf{A})\mathbf{\Phi}^T$, $m = 1, 2, \ldots, M$. And then LS update for $\mathbf{\Phi}$ is

$$\hat{\mathbf{\Phi}}^T = \begin{bmatrix} \hat{\mathbf{S}}^T D_1\left(\hat{\mathbf{A}}\right) \\ \hat{\mathbf{S}}^T D_2\left(\hat{\mathbf{A}}\right) \\ \vdots \\ \hat{\mathbf{S}}^T D_M\left(\hat{\mathbf{A}}\right) \end{bmatrix}^+ \begin{bmatrix} \tilde{\mathbf{Z}}_1 \\ \tilde{\mathbf{Z}}_2 \\ \vdots \\ \tilde{\mathbf{Z}}_M \end{bmatrix} \tag{20}$$

where $\tilde{\mathbf{Z}}_m, m = 1, 2, \ldots, M$ are the noisy slices. $\hat{\mathbf{A}}$ and $\hat{\mathbf{S}}$ denote previously obtained estimates of $\mathbf{A}$ and $\mathbf{S}$, respectively.

According to (16), (19) and (20), matrices $\mathbf{S}$, $\mathbf{A}$ and $\mathbf{\Phi}$ are updated with conditioned least squares, respectively. The matrix update will stop until convergence.

TALS algorithm is optimal when noise is additive i.i.d. Gaussian [36]. TALS algorithm has several advantages: it is easy to implement, guarantee to converge and simple to extend to higher order data. The shortcomings are mainly in the occasional slowness of the convergence process [37]. In this paper, we use the COMFAC algorithm [38] for trilinear decomposition. COMFAC algorithm is essentially a fast implementation of TALS, and can speeds up the LS fitting. COMFAC algorithm is essentially a fast implementation of TALS, and can speeds up the LS fitting. COMFAC compresses the three-way data into a smaller three-way data. After fitting the model in the compressed space, the solution is decompressed to the original space. This is followed by a few TALS steps in uncompressed space. Usually, the decompressed model is close to the LS solution, hence smaller TALS steps are sufficient for this refinement stage.

3.2. Identifiability

The k-rank concept is very important in the trilinear algebra.

*Definition***1** [30]: Consider a matrix $\mathbf{A} \in \mathbb{C}^{I \times J}$. If $\text{rank}(A) = r$, then $\mathbf{A}$ contains a collection of r linearly independent columns. Moreover, if every $l \leq J$ columns of $\mathbf{A}$ are linearly independent, but this does not hold for every $l+1$ columns, then $\mathbf{A}$ has k-rank $k_{\mathbf{A}} = l$. Note that $k_{\mathbf{A}} \leq \text{rank}(\mathbf{A})$, $\forall \mathbf{A}$.

*Theorem***1** [30]: $\mathbf{Z}_m = \mathbf{S}^T D_m(\mathbf{A})\mathbf{\Phi}^T$, $m = 1, 2, \ldots, M$, where $\mathbf{A} \in \mathbb{C}^{M \times K}$, $\mathbf{S} \in \mathbb{C}^{K \times N}$, $\mathbf{\Phi} \in \mathbb{C}^{P+1 \times K}$, considering that $\mathbf{A}$ is a matrix with Vandermonde characteristic, if

$$k_{\mathbf{S}^T} + \min(M + k_{\mathbf{\Phi}}, 2K) \geq 2K + 2 \tag{21}$$

then $\mathbf{A}$, $\mathbf{\Phi}$ and $\mathbf{S}$ are unique up to permutation and scaling of columns, that is to say, any other triple $\bar{\mathbf{A}}, \bar{\mathbf{\Phi}}, \bar{\mathbf{S}}$ that construct $\mathbf{Z}_m$, $m = 1, 2, \ldots, M$, is related to $\mathbf{A}$, $\mathbf{\Phi}$ and $\mathbf{S}$ via

$$\bar{\mathbf{A}} = \mathbf{A\Pi\Delta}_1, \;\; \bar{\mathbf{\Phi}} = \mathbf{\Phi\Pi\Delta}_2, \;\; \bar{\mathbf{S}}^T = \mathbf{S}^T\mathbf{\Pi\Delta}_3 \tag{22}$$

where $\mathbf{\Pi}$ is a permutation matrix, and $\mathbf{\Delta}_1, \mathbf{\Delta}_2, \mathbf{\Delta}_3$ are diagonal scaling matrices satisfying $\mathbf{\Delta}_1\mathbf{\Delta}_2\mathbf{\Delta}_3 = \mathbf{I}$.

Scale ambiguity and permutation ambiguity are inherent to the separation problem. This is not a major concern. Permutation ambiguity can be resolved by resorting to a priori or embedded information. The scale ambiguity can be resolved using automatic gain control, normalization and differential encoding/decoding.

In our present context, for source-wise independent source signals, $k_{\mathbf{S}^T} = \min(N, K)$; for source-wise independent delay, $k_{\mathbf{\Phi}} = \min(P + 1, K)$, and therefore, Eq. (21) becomes

$$\min(N, K) + \min((M + \min(P + 1, K), 2K) \geq 2K + 2 \tag{23}$$

For the received noisy signal, we use trilinear decomposition to get the estimated the direction matrix $\hat{\mathbf{A}}$ and the delay matrix $\hat{\mathbf{\Phi}}$, $\hat{\mathbf{A}} = \mathbf{A\Pi\Delta}_1 + \mathbf{N}_1$, $\hat{\mathbf{\Phi}} = \mathbf{\Phi\Pi\Delta}_2 + \mathbf{N}_2$, where $\mathbf{N}_1$, $\mathbf{N}_2$ are noises.

4. JOINT ANGLE AND FREQUENCY ESTIMATION

We can use trilinear decomposition to attain the direction matrix $\mathbf{A}$ and the delay matrix $\mathbf{\Phi}$, and then angle and frequency are estimated according to least square principle.

4.1. Frequency Estimation

Define the delay vector $\mathbf{g}(f_i)$ as

$$\mathbf{g}(f_i) = \left[1, e^{-j2\pi f_i \tau_1}, \ldots, e^{-j2\pi f_i \tau_P}\right]^T \tag{24}$$

$\mathbf{g}(f_i)$ is the ith column of the delay matrix $\mathbf{\Phi}$. According to (24), we get

$$\mathbf{h} = -\mathrm{imag}(\ln(\mathbf{g}(f_i))) \tag{25}$$

where ln(.) is natural logarithm; imag(.) is to get imaginary part of a complex number. Eq. (25) becomes $\mathbf{h} = [0, 2\pi f_i \tau_1, \ldots, 2\pi f_i \tau_{P-1}]^T$.

Assuming the estimated delay vector is $\hat{\mathbf{g}}(f_i)$ (the ith column of the estimated delay matrix $\hat{\mathbf{\Phi}}$). $\hat{\mathbf{g}}(f_i)$ is processed through normalization, which also resolves the scale ambiguity, and then normalized sequence is processed to attain $\hat{\mathbf{h}}$ according to (25). Finally we use lease squares principle to estimate f_i. Least squares fitting is

$$\mathbf{P}_1 \mathbf{b} = \hat{\mathbf{h}} \tag{26}$$

where

$$\mathbf{P}_1 = \begin{bmatrix} 1 & 0 \\ 1 & 2\pi\tau_1 \\ \vdots & \vdots \\ 1 & 2\pi\tau_P \end{bmatrix}, \quad \mathbf{b} = \begin{bmatrix} b_0 \\ f_i \end{bmatrix}$$

The least square solution for $\mathbf{b}$ is

$$\begin{bmatrix} \hat{b}_0 \\ \hat{f}_i \end{bmatrix} = \left(\mathbf{P}_1^T \mathbf{P}_1\right)^{-1} \mathbf{P}_1^T \hat{\mathbf{h}} \tag{27}$$

4.2. Angle Estimation

Define the direction vector for DOA θ_i as

$$\mathbf{a}(\theta_i) = \left[1, e^{-j2\pi d f_i \sin\theta_i / c}, \ldots, e^{-j2\pi(M-1) d f_i \sin\theta_i / c}\right]^T \tag{28}$$

According to (28)

$$\mathbf{u} = -\mathrm{imag}(\ln(\mathbf{a}(\theta_i))) \tag{29}$$

Eq. (29) becomes $\mathbf{u} = [0, 2\pi d f_i \sin\theta_i / c, \ldots, 2\pi d(M-1) f_i \sin\theta_i / c]^T$. We use least squares principle to estimate $\sin\theta_i$, and then estimate θ_i.

Assuming the estimated direction vector is $\hat{\mathbf{a}}(\theta_i)$ (the ith column of the estimated direction matrix $\hat{\mathbf{A}}$). The normalization for $\hat{\mathbf{a}}(\theta_i)$ is processed, and then normalized sequence is processed to attain $\hat{\mathbf{u}}$ according to (29). Finally we use lease squares principle to estimate $\sin\theta_i$. Least squares fitting is

$$\mathbf{P}_2 \mathbf{e} = \hat{\mathbf{u}} \tag{30}$$

where

$$\mathbf{P}_2 = \begin{bmatrix} 1 & 0 \\ 1 & 2\pi d\hat{f}_i/c \\ \vdots & \vdots \\ 1 & (M-1)2\pi d\hat{f}_i/c \end{bmatrix}, \quad \mathbf{e} = \begin{bmatrix} e_0 \\ e_1 \end{bmatrix}$$

where $\hat{f}_i$ is the estimated frequency through (27). e_1 is the estimated value of $\sin\theta_i$.

The least square solution for $\mathbf{e}$ is

$$\begin{bmatrix} \hat{e}_0 \\ \hat{e}_1 \end{bmatrix} = \left(\mathbf{P}_2^T \mathbf{P}_2\right)^{-1} \mathbf{P}_2^T \hat{\mathbf{u}} \tag{31}$$

DOA estimation is shown as follows

$$\hat{\theta}_i = \sin^{-1}(\hat{e}_1) \tag{32}$$

4.3. Joint Angle and Frequency Estimation Algorithm

In sum, trilinear decomposition-based joint angle and frequency estimation method for uniform linear array (Trilinear-JAFE) is presented in this paper. This algorithm firstly uses trilinear decomposition to attain the direction matrix and the delay matrix, and then uses least square principle to estimate frequency, finally estimates angle according to the estimated direction matrix and frequency.

5. SIMULATION RESULTS

Let $\tilde{\mathbf{X}}_p = \mathbf{A}D_{p+1}(\mathbf{\Phi})\mathbf{S} + \mathbf{W}_p$, the received noisy data, for $p = 0, 1, \ldots, P$, where $\mathbf{W}_p$ are the additive Gaussian white noise (AWGN) matrices. We define the sample SNR

$$\mathrm{SNR} = 10\log_{10} \frac{\sum_{p=0}^{P} \|\mathbf{A}D_{p+1}(\mathbf{\Phi})\mathbf{S}\|_F^2}{\sum_{p=0}^{P} \|\mathbf{W}_p\|_F^2} \, \mathrm{dB} \tag{33}$$

We present Monte Carlo simulations that are to assess the angle and frequency estimation performance of Trilinear-JAFE algorithm. The number of Monte Carlo trials is 1000. 16-element-uniform linear array is used in the simulations.

Note that

N is the number of snapshots.

K is the number of the sources.

P is the number of delay-outputs for received signal of array antennas.

Define $RMSE = \sqrt{\frac{1}{1000}\sum_{m=1}^{1000}[a_m - a_0]^2}$, where a_e is the estimated angle/frequency, and a_0 is the perfect angle/frequency.

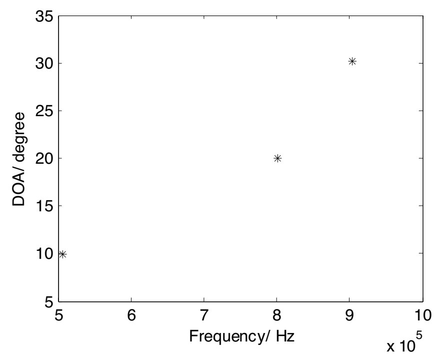

Figure 2. Angle-frequency scatter, SNR = 33 dB.

Simulation 1: The performance of our proposed algorithm is investigated. $P = 2$, $K = 3$ and $N = 50$ in this simulation. Their DOAs are 10°, 20° and 30°, and their carrier frequencies are 500 KHz, 800 KHz and 900 KHz. Fig. 2 shows the performance of our proposed algorithm with SNR = 33 dB. From Fig. 2, we find that our proposed algorithm works well.

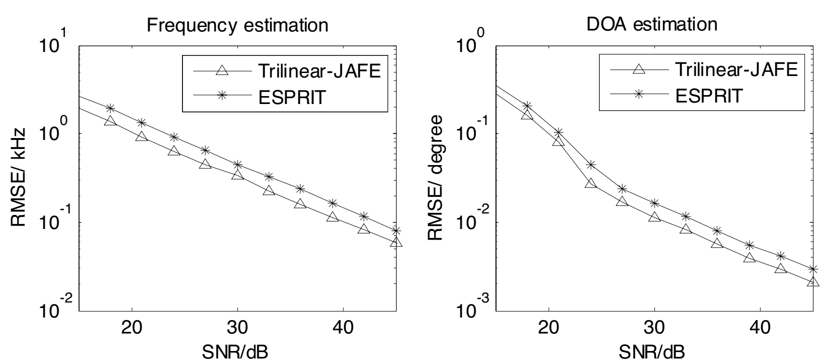

Figure 3. Angle-frequency estimation performance comparison.

Simulation 2: We compare our proposed algorithm with ESPRIT method. ESPRIT method is a multidimensional signal subspace methods and belongs to the same general class of subspace fitting methods. Trilinear-JAFE can be thought of as a generalization of ESPRIT. $K = 3$ and $N = 50$ in this simulation. From Fig. 3, we find that our proposed algorithm has better angle-frequency estimation performance than ESPRIT method.

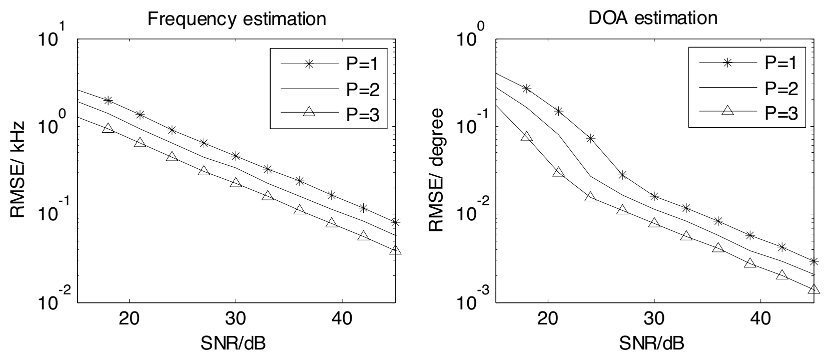

Figure 4. Angle-frequency estimation with different P.

Simulation 3: The performance of our proposed algorithm with different P is investigated. $K = 3$ and $N = 50$ in this simulation. Fig. 4 presents the frequency and angle estimation performance with different P. From Fig. 4, we also find that the angle-frequency estimation performance of Trilinear-JAFE algorithm is improved with P increasing. When P increases, that is to say delay diversity gain increases, the performance of Trilinear-JAFE algorithm is improved.

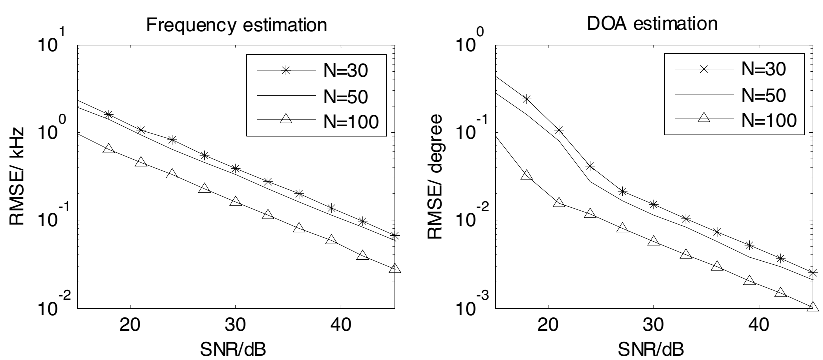

Figure 5. Angle-frequency estimation with different snapshot N.

Simulation 4: Trilinear-JAFE algorithm performance under different snapshots N is investigated in this simulation. $P = 2$ and $K = 3$ in this simulation. Fig. 5 shows the angle-frequency estimation performance under different N. From Fig. 5, we find that the angle-frequency estimation performance of Trilinear-JAFE algorithm is improved with N increasing.

Simulation 5: The performance of Trilinear-JAFE algorithm under different source number K is investigated in the simulation. $P = 2$, $N = 50$ in this simulation. The source number K is set 2, 3 and 4. Trilinear-JAFE algorithm has the different performance under different source number, as shown in Fig. 6. From Fig. 6, we find that angle and frequency estimation performance of Trilinear-JAFE algorithm degrades with the increasing of the source number K.

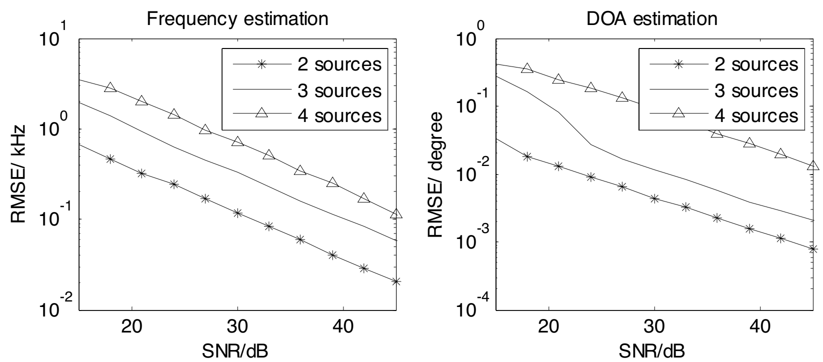

Figure 6. Angle-frequency estimation with different sources.

6. CONCLUSION

Our work links the uniform linear array parameter estimation problem to the trilinear model and derives a novel blind joint angle and frequency estimation algorithm. The proposed algorithm has better performance than ESPRIT. This method relies on a fundamental result of the uniqueness of low-rank three-way data decomposition. Our proposed algorithm is thought of as a generalization of ESPRIT, and has wider application. An advantage of our proposed algorithm over the classical subspace based algorithms, such as ESPRIT and MUSIC, is that it does not apply any eigenvalue decomposition to the cross spectral matrix or singular value decomposition to the received data. Our proposed method is an iterative algorithm, and it only requires fewer iterations for convergence.

ACKNOWLEDGMENT

This work is supported by NSF Grants (60801052) and Jiangsu NSF Grants (BK2007192). The authors wish to thank the anonymous reviewers for their valuable suggestions on improving this paper.

REFERENCES

1. Qu, Y., G. Liao, S.-Q. Zhu, and X.-Y. Liu, "Pattern synthesis of planar antenna array via convex optimization for airborne forward looking radar," *Progress In Electromagnetics Research*, PIER 84, 1–10, 2008.
2. Yang, Y., Y. Wang, and A. E. Fathy, "Design of compact vivaldi antenna arrays for UWB see through wall applications," *Progress In Electromagnetics Research*, PIER 82, 401–418, 2008.
3. Mouhamadou, M., P. Vaudon, and M. Rammal, "Smart antenna array patterns synthesis: Null steering and multi-user beamforming by phase control," *Progress In Electromagnetics Research*, PIER 60, 95–106, 2006.
4. Gustafsson, M., "RCS reduction of integrated antenna arrays with resistive sheets," *Journal of Electromagnetic Waves and Applications*, Vol. 20, No. 1, 27–40, 2006.
5. Liu, H.-X., H. Zhai, L. Li, and C.-H. Liang, "Progressive numerical method combined with MON for a fast analysis of large waveguide slot antenna array," *Journal of Electromagnetic Waves and Applications*, Vol. 20, No. 2, 183–192, 2006.
6. Fu, Y.-Q., Q.-R. Zheng, Q. Gao, and G. Zhang, "Mutual coupling reduction between large antenna arrays using electromagnetic bandgap (EBG) structures," *Journal of Electromagnetic Waves and Applications*, Vol. 20, No. 6, 819–825, 2006.
7. Li, B., B. Wu, and C.-H. Liang, "High gain circular waveguide array antenna using electromagnetic band-gap structure," *Journal of Electromagnetic Waves and Applications*, Vol. 20, No. 7, 955–966, 2006.
8. Guo J., J.-Y. Li, and Q.-Z. Liu, "Analysis of antenna array with arbitrarily shaped radomes using fast algorithm based on VSIE," *Journal of Electromagnetic Waves and Applications*, Vol. 20, No. 10, 1399–1410, 2006.
9. Psarros, I. and G. Fikioris, "Two-term theory for infinite linear array and application to study of resonances," *Journal of Electromagnetic Waves and Applications*, Vol. 20, No. 5, 623–645, 2006.

10. Lei, J., G. Fu, L. Yang, and D. M. Fu, "An omnidirectional printed dipole array antenna with shaped radiation pattern in the elevation plane," *Journal of Electromagnetic Waves and Applications*, Vol. 20, No. 14, 1955–1966, 2006.
11. Abdelaziz, A. A., "Improving the performance of an antenna array by using radar absorbing cover," *Progress In Electromagnetics Research Letters*, Vol. 1, 129–138, 2008.
12. Xiao, S.-Q., J. Chen, X.-F. Liu, and B.-Z. Wang, "Spatial focusing characteristics of time reversal UWB pulse transmission with different antenna arrays," *Progress In Electromagnetics Research B*, Vol. 2, 223–232, 2008.
13. Landesa, L., I. T. Castro, J. M. Taboada, and F. Obelleiro, "Bias of the maximum likelihood DOA estimation from inaccurate knowledge of the antenna array response," *Journal of Electromagnetic Waves and Applications*, Vol. 21, No. 9, 1205–1217, 2007.
14. Lizzi, L., F. Viani, M. Benedetti, P. Rocca, and A. Massa, "The M-DSO-Esprit method for maximum likelihood DOA estimation," *Progress In Electromagnetics Research*, PIER 80, 477–497, 2008.
15. Gu, Y.-J., Z.-G. Shi, K. S. Chen, and Y. Li, "Robust adaptive beamforming for steering vector uncertainties based on equivalent DOAs method," *Progress In Electromagnetics Research*, PIER 79, 277–290, 2008.
16. Lie, J. P., B. P. Ng, and C. M. See, "Multiple UWB emitters DOA estimation employing time hopping spread spectrum," *Progress In Electromagnetics Research*, PIER 78, 83–101, 2008.
17. Mukhopadhyay, M., B. K. Sarkar, and A. Chakrabarty, "Augmentation of anti-jam GPS system using smart antenna with a simple DOA estimation algorithm," *Progress In Electromagnetics Research*, PIER 67, 231–249, 2007.
18. Harabi, F., H. Changuel, and A. Gharsallah, "Direction of arrival estimation method using a 2-L shape arrays antenna," *Progress In Electromagnetics Research*, PIER 69, 145–160, 2007.
19. Changuel, H., F. Harabi, and A. Gharsallah, "2-L-shape two-dimensional arrival angle estimation with a classical subspace algorithm," *Progress In Electromagnetics Research*, PIER 66, 301–315, 2006.
20. Djeddou, M., A. Belouchrani, and S. Aouada, "Maximum likelihood angle-frequency estimation in partially known correlated noise for low-elevation targets," *IEEE Trans. on Signal Processing*, Vol. 53, No. 8, 3057–3064, 2005.

21. Zoltowski, M. D. and C. P. Mathews, "Real-time frequency and 2-D angle estimation with sub-Nyquist spatio-temporal sampling," *IEEE Trans. on Signal Processing*, Vol. 42, 2781–2794, 1994.
22. Haardt, M. and J. A. Nossek, "3-D unitary ESPRIT for joint angle and carrier estimation," *Proc. ICASSP*, 255–258, Munich, Germany, 1997.
23. Lemma, A. N., A.-J. van der Veen, and E. F. Deprettere, "Joint angle frequency estimation using multi-resolution ESPRIT," *Proc. ICASSP*, Vol. 4, 1957–1960, Seattle, WA, 1998.
24. Lemma, A. N., A. J. van der Veen, and E. F. Deorettere, "Analysis of joint angle-frequency estimation using ESPRIT," *IEEE Trans. on Signal Processing*, Vol. 51, No. 5, 1264–1283, 2003.
25. Chen, H., Y. Wang, and Z. Wu, "Frequency and 2-D angle estimation based on uniform circular array," *2003 IEEE International Symposium on Phased Array Systems and Technology*, 547–552, 2003.
26. Fu, T., S. Jin, and X. Gao, "Joint 2-D angle and frequency estimation for uniform circular array," *2006 International Conference on Communications, Circuits and Systems Proceedings*, Vol. 1, 230–233, 2006.
27. Wang, S. and X. Zhou, "Direction-of-arrival and frequency estimation in array signal processing," *Journal of Shanghai Jiaotong University*, Vol. 33, No. 1, 40–42, 1999.
28. Jia, W., M. Yao, and J. Song, "Joint frequency, two dimensional arrival angles estimations via marked signal subspace," *The 8th International Conference on Signal Processing*, Vol. 1, 16–20, 2006.
29. Lin, C., W. Fang, K. Wu, and J. Lin, "Fast algorithm for joint azimuth and elevation angles, and frequency estimation via hierarchical space-time decomposition," *IEEE International Conference on Acoustics, Speech and Signal Processing*, Vol. 2, 1061–1064, 2007.
30. Kruskal, J. B., "Three-way arrays: Rank and uniqueness of trilinear decompositions, with application to arithmetic complexity and statistics," *Linear Algebra Applicat.*, Vol. 18, 95–138, 1977.
31. Pham, T. and J. Mocks, "Beyond principal component analysis: A trilinear decomposition model and least squares estimation," *Psychometrika*, Vol. 57, No. 2, 203–215, 1992.
32. Wu, H., R. Yu, and K. Oguma, "Trilinear component analysis in modern analytical chemistry," *Anal. Sci.*, Vol. 17, 1483–1486,

2001.

33. Wise, B. M., N. B. Gallagher, S. W. Butler, D. D. White, and G. G. Barna, "A comparison of principal component analysis, multiway principal component analysis, trilinear decomposition and parallel factor analysis for fault detection in a semiconductor etch process," *Journal of Chemometrics*, Vol. 13, 379–396, 1999.
34. Henrion, R. and C. A. Andersson, "A new criterion for simple-structure core transformations in N-way principal components analysis," *Chemom. Intell. Lab. Syst.*, Vol. 47, 189–204, 1999.
35. De Lathauwer, L., B. de Moor, and J. Vandewalle, "Computation of the canonical decomposition by means of a simultaneous generalized schur decomposition," *SIAM J. Matrix Anal. Appl.*, Vol. 26, No. 2, 295–327, 2004.
36. De Lathauwer, L., "A link between the canonical decomposition in multilinear algebra and simultaneous matrix diagonalization," *SIAM J. Matrix Anal. Appl.*, Vol. 28, No. 3, 642–666, 2006.
37. Vorobyov, S. A., Y. Rong, N. D. Sidiropoulos, and A. B. Gershman, "Robust iterative fitting of multilinear models," *IEEE Trans. on Signal Processing*, Vol. 53, No. 8, 2678–2689, 2005.
38. Bro, R., N. D. Sidiropoulos, and G. B. Giannakis, "A fast least squares algorithm for separating trilinear mixtures," *International Workshop Independent Component Analysis and Blind Signal Separation*, 289–294, Aussois, France, 1999.